



Available online at [www.sciencedirect.com](http://www.sciencedirect.com)

**ScienceDirect**

Procedia Environmental Sciences 33 (2016) 583 – 599

**Procedia**  
Environmental Sciences

The 2<sup>nd</sup> International Symposium on LAPAN-IPB Satellite for Food Security and Environmental Monitoring 2015, LISAT-FSEM 2015

## The seasonal variability of sea surface temperature and chlorophyll-a concentration in the south of Makassar Strait

Bisman Nababan\*, Novilia Rosyadi, Djisman Manurung, Nyoman M. Natih, and Romdonul Hakim

*Department of Marine Science and Technology, Bogor Agricultural University, Jl. Lingkar Akademik, Kampus IPB Darmaga, Bogor 16680, Indonesia*

---

### Abstract

The sea surface temperature (SST) and chlorophyll-a (Chl-a) variabilities in the south of Makassar Strait were mostly affected by monsoonal wind speed/directions and riverine freshwater inflows. The east-southeast (ESE) wind (May–October) played a major role in an upwelling formation in the region starting in the southern tip of the southern Sulawesi Island. Of the 17 years time period, the variability of the SST values ranged from 25.7°C (August 2004) - 30.89°C (March 2007). An upwelling initiation typically occurred in early May when ESE wind speed was at <5 m/s, a fully developed upwelling event usually occurred in June when ESE wind speed reached ≥5 m/s, whereas the largest upwelling event always occurred in August of each year. Upwelling event generally diminished in September and terminated in October. At the time of the maximum upwelling events (August), the formation of upwelling could be observed up to about 330 km toward the southwest of the southern tip of the Sulawesi island. Interannually, El Niño Southern Oscillation (ENSO) intensified the upwelling event during the east season through an intensification of the ESE wind speed.

© 2016 The Authors. Published by Elsevier B.V. This is an open access article under the CC BY-NC-ND license (<http://creativecommons.org/licenses/by-nc-nd/4.0/>).

Peer-review under responsibility of the organizing committee of LISAT-FSEM2015

**Keywords:** SST; Chl-a concentration; upwelling; east season; ENSO; Makassar Strait.

---

\* Corresponding author. Tel.: +62-813-1732-5601.

E-mail address: [bisman@ipb.ac.id](mailto:bisman@ipb.ac.id); [simson\\_naban@yahoo.com](mailto:simson_naban@yahoo.com)

## 1. Introduction

The south of Makassar Strait lies between the southern part of Sulawesi and the southeastern part of Kalimantan (Borneo). The Strait is connected to the Pacific Ocean in the north through the Celebes Sea, to the Java Sea in the west, to the Flores Sea in the east, and to the Indian Ocean in the south via the Lombok Strait (between the eastern Bali island and western Lombok island), the Alas Strait (between the eastern Lombok island and western Sumbawa island), and the Sape Strait (between eastern Sumbawa island and the Komodo island). Due to its strategic location, the variability of chlorophyll-a concentration (Chl-a) and sea surface temperature (SST) of the south of Makassar Strait is generally affected by: (1) monsoonal winds [1,2,3]; (2) deep-sea exchange of water masses from the Pacific Ocean through Indonesian Through Flow (ITF) via Celebes Sea [4,5,6,7,8]; (3) transport of low salinity (buoyant) surface water from the Java Sea during Northwest Monsoon (January–March) and more saline (less buoyant) surface water from the Flores Sea during Southeast Monsoon (July–September) [9]; (4) upwelling event during Southeast Monsoon [1,10,11]; (5) climate anomalies such as El Nino Southern Oscillation (ENSO) and Dipole Indian Mode [12,13]; and (6) fresh water inflows from rivers in southeast Kalimantan and south Sulawesi [14].

The general pattern of the surface ocean currents (Ekman layer) in the south of Makassar Strait is influenced by monsoonal wind variability. During the Southeast Monsoon, also called the East Season (May–August), the surface wind in general comes from the southeast direction causing the Ekman layer in the southern part of Makassar Strait to flow in southwest direction away from the coastal region and to cause an upwelling event in the region. During the Northwest Monsoon also called West Season (November–February), the surface wind in general comes from northwest direction causing the Ekman layer in the southern part of the Makassar Strait to flow in the northeast direction heading toward the coastal region and causing a downwelling event in the region [11, 15, 16,17]. Irregular wind directions typically occur during the first transitional season (March–April) and the second transitional season (September–October).

The ITF maximum transport flowing through the Makassar Strait at the entrance and exit is expected to occur at different times, so that the water mass storage occurs some time along the Makassar Strait. The ITF maximum transport passing through the deep Labani channel (located in the south of Makassar Strait) occurs during the Southeast Monsoon/East Season (July–September) and is at a minimum during October–December (second transitional and early west seasons) [4,6,18]. The maximum transport of ITF during the east season intensifies the upwelling process in the south of Makassar Strait [1].

Upwelling occurs regularly in south of Makassar Strait during the Southeast Monsoon/East Season particularly in August [1, 2, 8, 14, 11, 19, 20, 21, 22]. Based on measurements of SST, chlorophyll-a concentration (Chl-a), and wind satellite data acquired in 2004, Setiawan and Kawamura [11] reported that the south of Makassar Strait region was covered by warm water with a sea surface temperature (SST) of about 29–30°C during west season and a relatively low Chl-a ( $\sim 0.3 \text{ mg m}^{-3}$ ). However, in August, the Chl-a increased to a maximum of  $1.3 \text{ mg m}^{-3}$ . Based on SeaWiFS, AVHRR, Quicscat satellite data acquired over the period May 1999–Sep 2004, Habibi *et al.* [2] found that a Chl-a bloom along south of Sulawesi island waters was started in May and reached its maximum in August ( $1.1 \text{ mg/m}^3$ ) before it weakened in September. They concluded that the southeasterly monsoon winds were responsible for the coastal upwelling formation along the south of Sulawesi Island. Atmadipoera *et al.* [19] also reported that high-salinity surface water from the south of Makassar Strait was advected into Java Sea during the southeast monsoon (SEM) period indicating an upwelling evidence in the region of the south of Makassar Strait.

Previous studies were generally conducted over a short period of time, rather than aiming to understand the spatial and temporal distribution and variability over a prolonged period of time. Moreover, information of the extent, initiation, and termination dates of the upwelling events in the south of Makassar Strait region is still limited. Therefore, a study on the seasonal variability of sea surface temperature and Chl-a spatially and temporally using satellite and field data over a prolonged period of time was urgently needed.

The objectives of this research were to determine the seasonal and factor affecting the variability of the SST and Chl-a, to determine the extent, initiation, and termination of the upwelling events, and to determine the interannual variabilities of SST and Chl-a in the south of Makassar Strait.

## 2. Data and Methods

### 2.1. Study area

The research location was the south of Makassar Strait located at 2.7-8.1°S and 115.9-120°E (yellow box in Fig. 1). To determine variabilities and distributions of SST and Chl-a along the south of Makassar Strait spatially and temporally, we subjectively selected 4 (four) sampling areas representing four important regions along the strait i.e., (1) region near to the upwelling source centered at 6°S, 119°E, (2) western region of upwelling source centered at 6°S, 117°E, (3) northern region of the strait centered at 3.5°S, 118°E, and (4) southeast region of upwelling source centered at 7°S, 117°E (Fig. 1). By having these four sampling areas, we expected that we were able to determine the variabilities and distribution patterns of SST and Chl-a along the strait and also the impact of upwelling event and local rivers run off to the variabilities and distribution patterns of SST and Chl-a along the strait. From these four boxes, we extracted and analyzed SST and Chl-a of the satellite data to determine their spatial and temporal variabilities. The pixel size of each sampling area was 0.5°x0.5°.

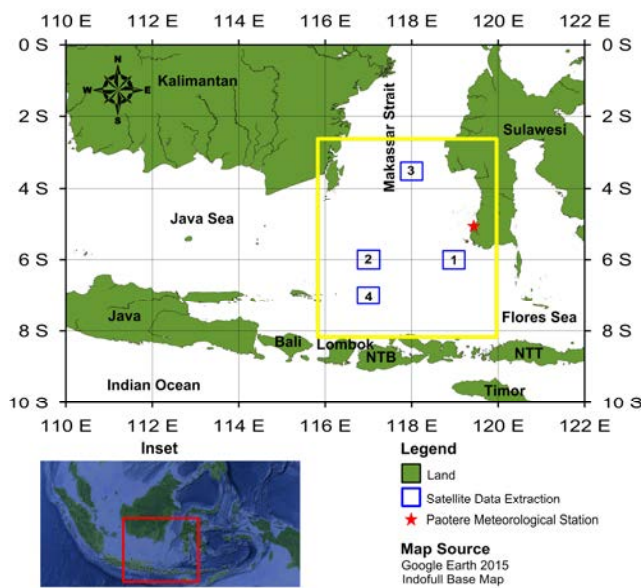


Fig. 1. Research study location of the south of Makassar Strait (indicated by yellow rectangle). The four boxes indicate the locations where SST and Chl-a extracted from satellite data. The inset shows the study location on the Indonesian map. Rainfall data were obtained from Paotere Meteorological Station.

### 2.2. Data and analyses

Monthly mean Chl-a data were extracted from Ocean Color SeaWiFS and MODIS Aqua satellites level 3 composites of 9 x 9 km<sup>2</sup> spatial resolution. The Chl-a data were extracted from 0.5° x 0.5° pixel size of the four selected sampling areas for the period of January 1998 - December 2010 for SeaWiFS and January 2011 - December 2014 for MODIS Aqua. Both data were extracted using Giovanni - Interactive Visualization and Analysis - GES DISC: Goddard Earth Sciences, Data and Information Services Center (<http://disc.sci.gsfc.nasa.gov/> Giovanni [23]. SeaWiFS Chl-a was estimated using the Ocean Chlorophyll 4-band algorithm version 4 (OC4v4) [24], while MODIS Chl-a was estimated applying the Ocean Chlorophyll MODIS algorithm (OC3M).

To eliminate erroneous Chl-a estimate data specifically due to the impact of particulate suspended matter, bottom reflectance, and case-2 water condition, we only used “valid” Chl-a data from both SeaWiFS and MODIS satellites data within the range of  $0 < \text{Chl-a} \leq 10 \text{ mg/m}^3$ . We chose this “valid” Chl-a data range because based on pre-analyses SeaWiFS and MODIS data of the four selected areas, we found that Chl-a values were generally in the range of  $0-10 \text{ mg/m}^3$ . Other previous field measurements also showed that the values of Chl-a measurements were within the range of  $0-10 \text{ mg/m}^3$  [21, 22].

There was a time period overlap between SeaWiFS and MODIS Chl-a data availability i.e., July 2002 – December 2010. We performed data comparison between the two and found that MODIS data was in general slightly lower than SeaWiFS data. Therefore, we decided to use SeaWiFS data for the period of January 1998–December 2010 and MODIS data for the period of January 2011–December 2014. For variability data analyses, we calculated anomaly of Chl-a concentration with the following approaches:

$$\frac{X_i - X_1}{X_1} \quad (1)$$

$$\frac{X_i - X_2}{X_2} \quad (2)$$

Where  $X_i$  is the monthly SeaWiFS or MODIS Chl-a in i-month,  $X_1$  is the monthly average of SeaWiFS Chl-a data for the period of January 1998 – December 2010, and  $X_2$  is the monthly average of the MODIS Chl-a data for the period of July 2002–December 2014.

Monthly SST Pathfinder v5 data were extracted from NOAA-AVHRR satellite imagery of  $4 \times 4 \text{ km}^2$  spatial resolution within  $0.5^\circ \times 0.5^\circ$  pixel size of the four selected sample areas for the period of January 1998 – December 2009 and were obtained from the National Aeronautics and Space Administration (NASA) website (<http://www.podaac.jpl.nasa.gov>). Sea surface temperature data were estimated using Pathfinder algorithm v5 [25]. Due to the availability of the Pathfinder SST data only until December 2009, we, therefore, use monthly SST data from both Aqua and Terra MODIS day and night of 11 micron for the period of January 2010 – December 2014 utilizing the Giovanni online data system, developed and maintained by the NASA GES DISC (<http://disc.sci.gsfc.nasa.gov/giovanni>) [23]. All day and night of Aqua and Terra MODIS monthly SST data were later averaged to produce monthly mean SST data.

To avoid erroneous SST data specifically due to the effect of thin cloud, water vapor, and sun glint, we only used valid SST data from both NOAA-AVHRR and MODIS satellites data within the range of  $20 < \text{SST} \leq 32^\circ\text{C}$ . We chose this valid SST data range because based on several previous field measurements the values of sea surface temperature in this region never exceeded this range.

There was a time period overlap between AVHRR Pathfinder and MODIS SST data availability i.e., July 2002 – December 2009. We performed data comparison between the two and found that MODIS SST data was in general slightly lower than AVHRR Pathfinder SST data. Therefore, we decided to use AVHRR Pathfinder SST data for the period of January 1998–December 2009 and MODIS SST data for the period of January 2010–December 2014. For variability data analyses, we calculated anomaly of SST with the following approaches:

$$\frac{Y_i - Y_1}{Y_1} \quad (3)$$

$$\frac{Y_i - Y_2}{Y_2} \quad (4)$$

Where  $Y_i$  is monthly AVHRR or MODI SST value in i-month,  $Y_1$  is the monthly average of SST of AVHRR Pathfinder data for the period of January 1998 – December 2009, and  $Y_2$  is the monthly average of SST of MODIS data for the period of July 2002–December 2014.

The monthly average rainfall (mm) for the period January 1998–December 2014 was taken from the Meteorological Station Paotere, Makassar, South Sulawesi located at the coordinates of  $5^\circ 6' 37.5''\text{S}$  and  $119^\circ 25' 11.5''\text{E}$ .

Daily wind data in the study area taken at 00:00, 06:00, 12:00, and 18:00 at 10 m above sea level with a spatial resolution of  $1.5^\circ \times 1.5^\circ$  in the period January 1998 – December 2014 were obtained from European Centre for Medium - Range Weather Forecasts (ECMWF) website (<http://www.ecmwf.int>). The wind data were averaged into monthly average to determine the wind direction and speed.

### 2.3. Interannual analyses

For analyses of the interannual variabilities of SST and Chl-a, we used the Southern Oscillation Index (SOI) (air pressure difference between Tahiti and Darwin) as an indicator of El Niño and La Niña events. During SOI negative, the SST of the tropical eastern Pacific Ocean is relatively higher than the normal conditions, and the vice versa for the positive SOI. The months included in the category El Niño Southern Oscillation (ENSO) were within the SOI

values  $\leq -10$ , while the months included in the category of La Niña were within the SOI values  $\geq 10$  [26]. For this study, we used five month running mean of monthly SOI index values of  $< -5$  to be categorized as an ENSO month. Based on this category, we grouped the months during the ENSO month of each year (Table 1). Monthly SOI index data were obtained from the Australian Bureau of Meteorology (<http://www.bom.gov.au/climate/current/soi>).

Table 1. List of ENSO months during the study period.

Year	ENSO months during the year
1998	January, February, March, April, May
1999	None
2000	None
2001	None
2002	May, June, July, August, September, October, November, December
2003	January, February, March, April, May
2004	June, August, September, October, December
2005	January, February, March, April, June
2006	July, August, September, October, November, December
2009	October, November, December
2010	January, February
2012	June
2013	None
2014	August, September, October, November, December

### 3. Results and Discussion

#### 3.1. SST temporal and spatial variability

Based on AVHRR Pathfinder and MODIS monthly mean SST values in the south of Makassar Strait for the period of January 1998 to December 2014 (17 years time period), the annual minimum values of each year were generally observed during the East Season (August) and the annual maximum values of each year were observed during the West Season (December–February) or the first transitional season (March–April). Overall, the monthly mean SST values ranged from 25.73°C (sampling area1, August 2004) to 30.89°C (sampling area1, March 2007). In average, the minimum monthly mean SST values were observed in August, while the maximum values were found in November or April (Fig. 2).

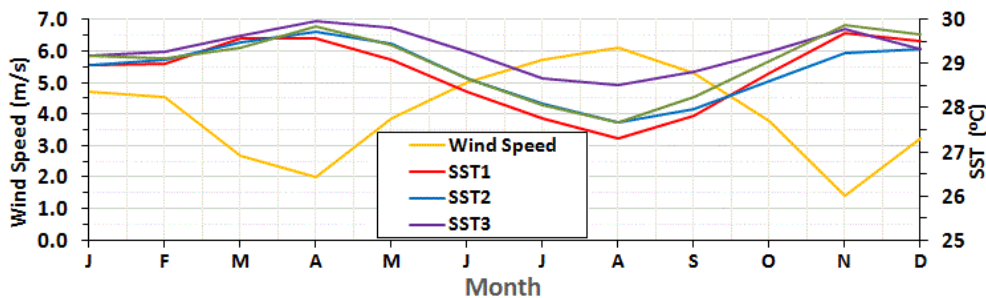


Fig. 2. Seasonal cycle of the monthly mean SST at the four selected sampling areas and seasonal cycle of the average monthly wind speed (extracted from sampling area1) in the south of Makassar Strait.

On the annual mean basis, seasonal monthly mean SST values were observed within the four sampling areas. In general, relatively lower monthly mean SST values (negative anomalies) were generally found during the East Season (May–August) and the second transitional season (September–October), while relatively higher monthly mean SST values (positive anomalies) were observed during the early West Season (November) and the first transitional season (April) (Fig. 2). The relatively lower monthly mean SST values (negative anomalies) during east and second transitional seasons occurred coherently with the relatively higher east-southeasterly (ESE) wind speed, while higher monthly mean SST values (positive anomalies) occurred during the relatively low west-northwesterly (WNW) wind (Fig. 2).

We found that east-southeasterly (ESE) wind occurred during the months May–October, while west-northwesterly (WNW) wind occurred during the months December–March in the south of Makassar Strait (Fig. 3). Our findings have little discrepancies to previous findings that the SE wind occurs in this region during the months May–October and the NW wind occurs during the months December–March [2, 7, 10]. The ESE wind which reached its maximum speed during August in each year was believed to be a major factor causing cooling SST during east and second transitional seasons in the south of Makassar Strait specifically near the southern tip of Sulawesi Island [1, 2, 7, 10]. A detailed discussion of the wind factor can be found in section 3.4.

Spatially, during the west season (November–February) and first transitional season (March–April), monthly mean SST values in general showed positive anomalies (Fig. 3, Fig. 4). In some events in the month of January, February, and March, we found negative anomalies of monthly mean SST values (Fig. 4, middle panel and lower left panel). The negative anomalies here were due to some erroneous SST values as a result of high cloud cover or high water vapor during these months. High cloud cover (90–96%) can frequently be observed over Indonesian waters during this time period [27].

During the east season (May–August) and the second transitional season (September–October), the monthly mean SST values in general showed negative anomalies which originated from the southern tip of Sulawesi island and later extended toward west and southwest direction (Fig. 3, Fig. 5). Negative anomalies of monthly mean SST values during these seasons were caused by ESE winds blowing over this region and causing upwelling events. During these times, the region also experienced dry season or relatively low cloud cover so that little atmospheric effects could cause erroneous satellite SST estimation [29, 30].

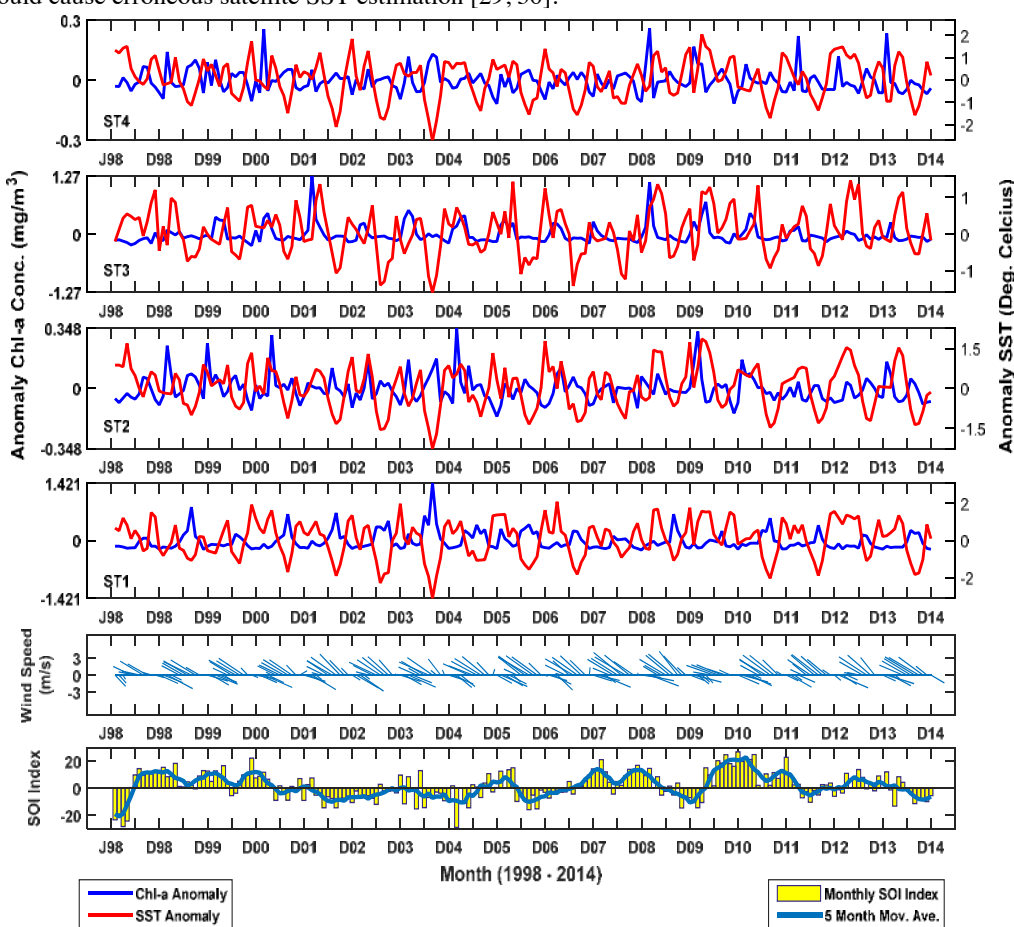


Fig. 3. Plots of SOI, wind speed at 10 m extracted from sampling area1, monthly mean SST and Chl-a anomalies for four selected study areas.  
Note: J98 and D98 in x-axis denoted for January 1998 and December 1998. For clarity, scales on the left and right y-axis are not identical.

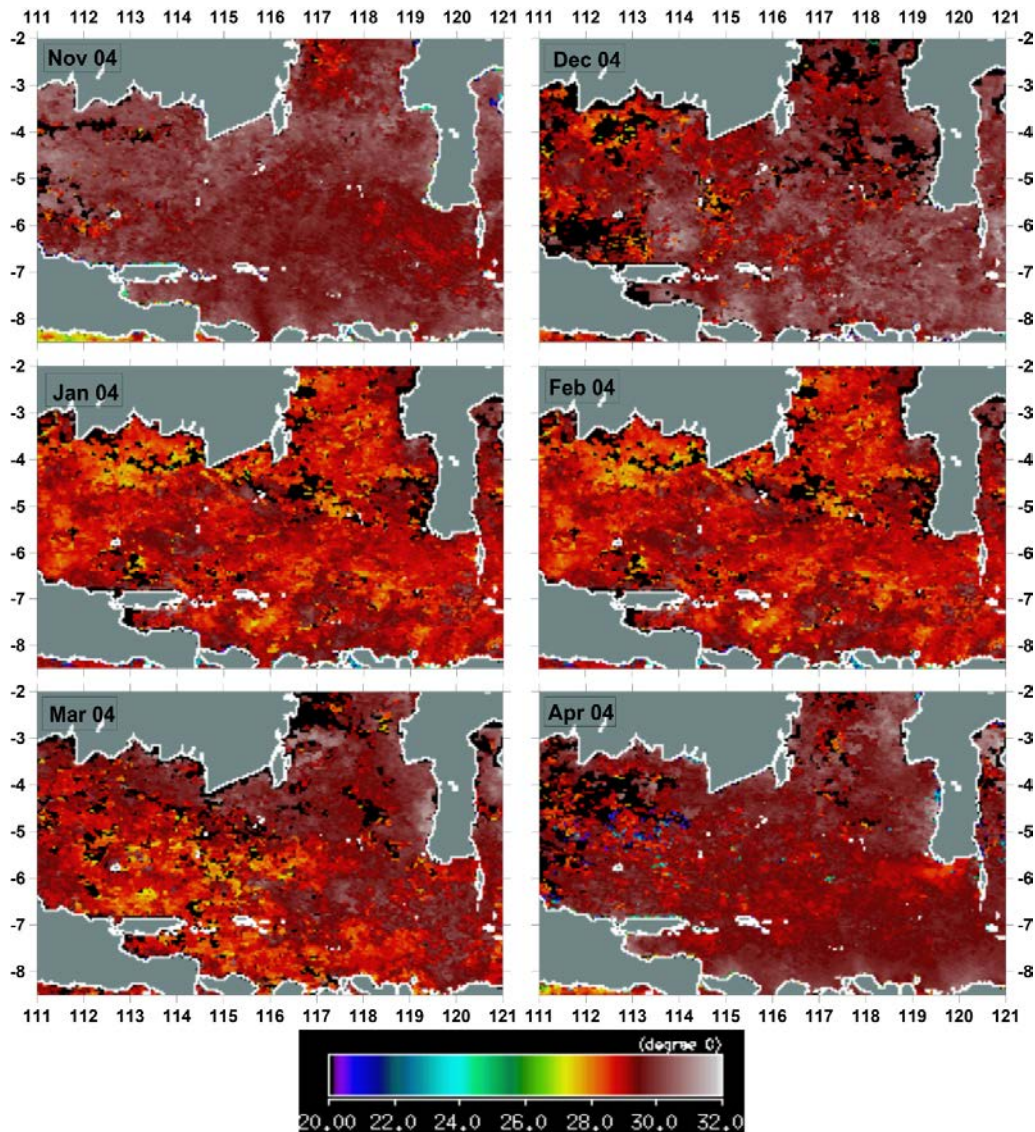


Fig. 4. Example of spatial monthly mean SST distribution during west season (Nov-Feb 2004, upper and middle panels) and first transitional season (Mar-Apr 2004, bottom panel).

Negative anomalies of monthly mean SST values during the east and second transitional seasons usually started in May, reached its minimum in August, and terminated in October. The largest upwelling event of 17 years time period occurred in August 2004 with the monthly mean SST anomaly of  $-3.09^{\circ}\text{C}$  ( $25.7^{\circ}\text{C}$ ) and the upwelling region was extended about 330 km from the southern tip of the Sulawesi island toward the southwest of the region (Fig. 5). This SST value was almost similar to field measurements in August 1971 and 1974 by Ilahude [23] that the upwelling in the south of Makassar Strait with a homogeneous layer of 50 m deep of colder water mass of  $26\text{-}27^{\circ}\text{C}$ . The upwelling event occurred during these seasons was also consistent with some previous studies [1, 2, 5, 7, 9, 12, 14, 21, 30].

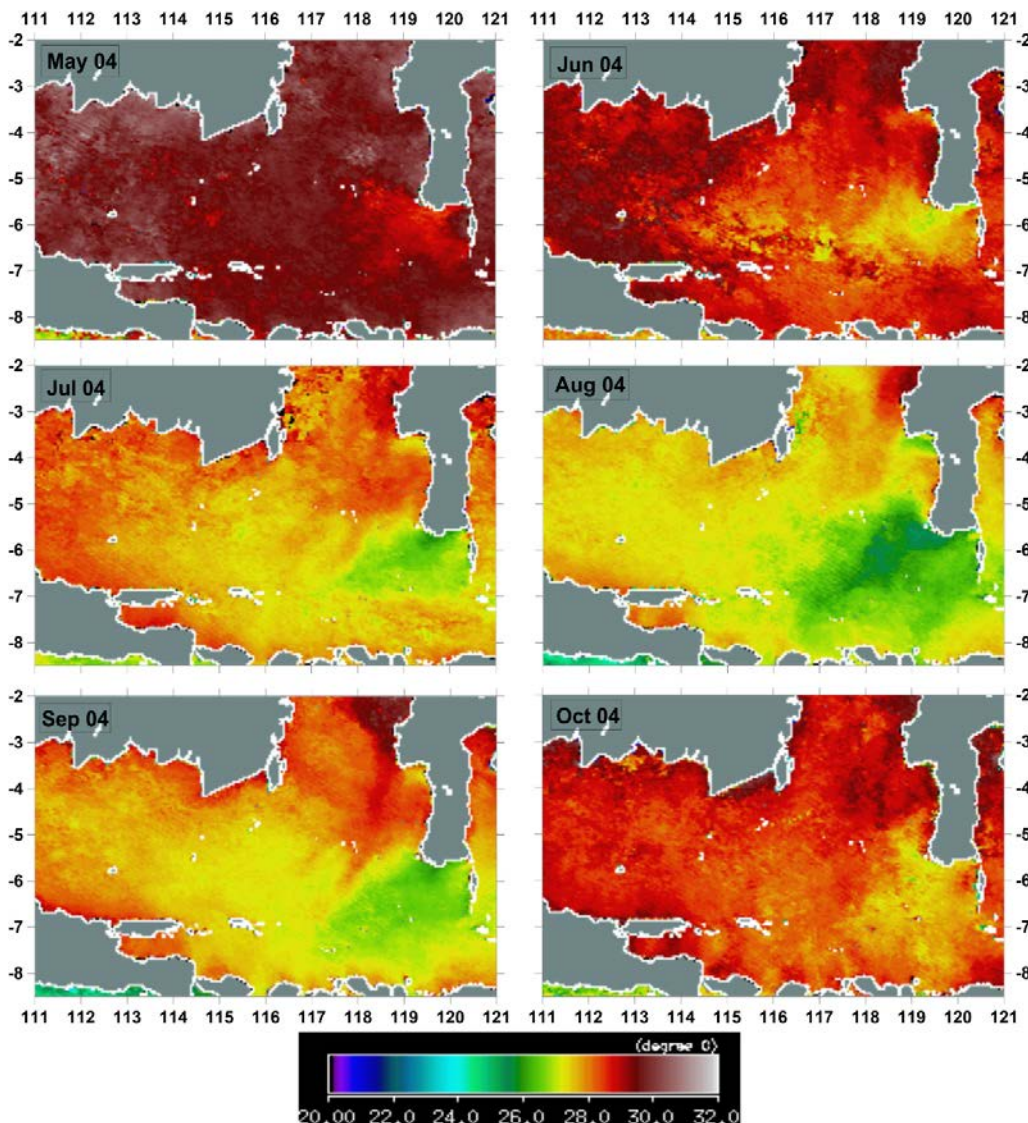


Fig. 5. Example of spatial monthly mean SST distribution during east season (May-Aug 2004, upper and middle panels) and second transitional season (Sep-Oct 2004, bottom panel).

### 3.2. Chlorophyll-a concentration spatial and temporal variability

Based on monthly mean Chl-a from SeaWiFS and MODIS satellite data for the period of January 1998 to December 2014, Chl-a in the south of Makassar Strait ranged from 0.09 mg m<sup>-3</sup> (December 2005, sampling area2) to 1.782 mg m<sup>-3</sup> (August 2004, sampling area1) with average values range between 0.216 mg m<sup>-3</sup> and 0.374 mg m<sup>-3</sup> (Table 2). The annual minimum values were generally observed during the early west season (November and December), while the annual maximum values were found during the east season (August) or late west season (February) and early first transitional season (March) (Table 2, see also Fig. 3).

Table 2. Minimum, maximum, and average values of monthly mean Chl-a ( $\text{mg m}^{-3}$ ) of the four selected sampling areas.

	Sta1	Sta2	Sta3	Sta4
Minimum	0.128 (Dec-08)	0.098 (Dec-05)	0.149 (Nov-00)	0.106 (Dec-05)
Maximum	1.782 (Aug-04)	0.609 (Feb-05)	1.667 (Feb-02)	0.483 (Feb-09)
Average	0.345	0.249	0.374	0.216

On the annual average basis, the four selected regions did not exhibit a consistent pattern of seasonality for monthly mean Chl-a values. The sampling area1 located near to the southern tip of Sulawesi Island and the initial location for upwelling event was the only location which exhibited clear seasonal pattern with negative relationship with monthly mean SST. In this region, relatively higher monthly mean Chl-a were observed during the east and second transitional seasons with maximum in August, while the lower values were observed during the west season (Fig. 6, lower panel). This indicated that monthly mean Chl-a variability in this region was mostly affected by variability of upwelling event.

For the sampling area2 (west site of study region), sampling area3 (northern site of study region), and sampling area4 (southwest site of the study region), we observed a semi-annual seasonal pattern with the first maximum value of monthly mean Chl-a during late west season (February) and the second peak in late east season (August) (Fig. 6, see also Fig. 3). The relatively high monthly mean Chl-a in the late west season in these regions was affected by rainy season during the west season and caused high freshwater and nutrients discharge into the coastal waters around the southeast Kalimantan island and later transported by surface current toward south and southeast regions of the Kalimantan island. This evident can be observed from monthly mean Chl-a spatial distribution (Feb 04 in Fig. 7). Meanwhile, the positive anomalies of monthly mean Chl-a in August was clear due to upwelling event initiated at the tip of southern Sulawesi island (Aug 04 in Fig. 8). Similar results were also confirmed with previous field measurements [14,31] that higher nutrient contents (phosphate, nitrate, and Chl-a) in the surface layer of the south of Makassar Strait were observed due to upwelling phenomena during the east and second transitional seasons.

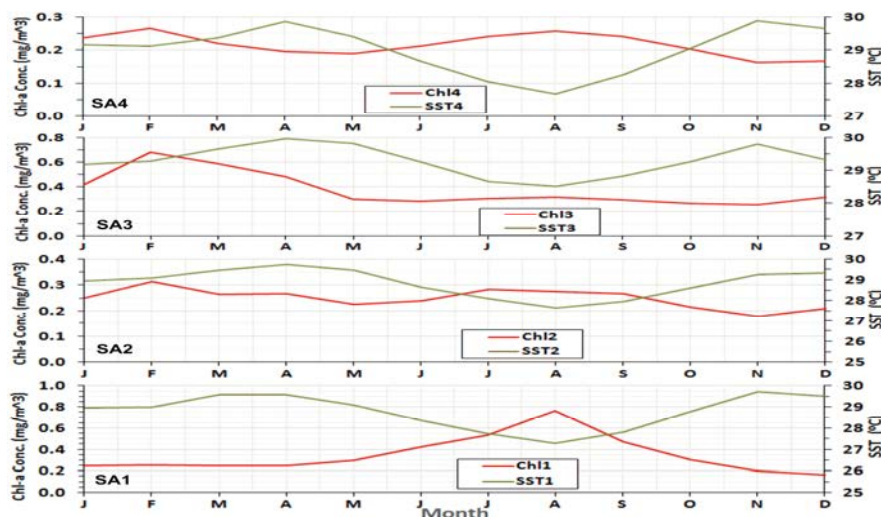


Fig. 6. Seasonal cycle of monthly mean Chl-a and SST values of the four selected sampling areas in the south of Makassar Strait. Note that the left y-axis and the right y-axis in each sampling areas do not have the same scale.

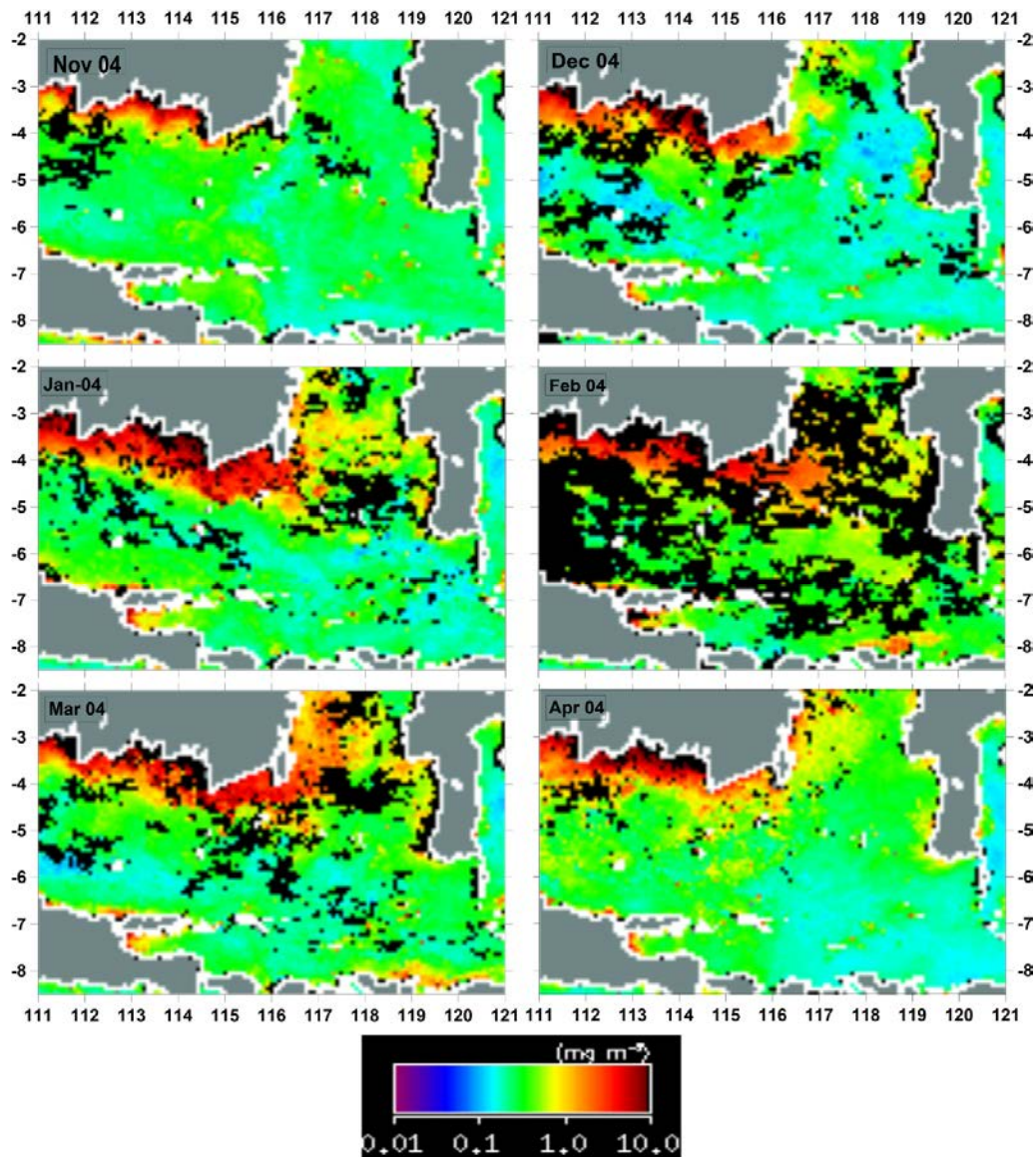


Fig. 7. Example of spatial monthly mean Chl-a distribution during west season (top and middle panels) and first transitional season (bottom panel).

Upwelling phenomena occurred during the east and second transitional seasons seemed providing no impact affecting the variability of monthly mean Chl-a in the study area 3 (northern site of the study region). The ESE wind blew in this region during these seasons produced southwestward Ekman surface current that prohibited upwelling water from the southern tip of Sulawesi island to be transported toward northwest direction.

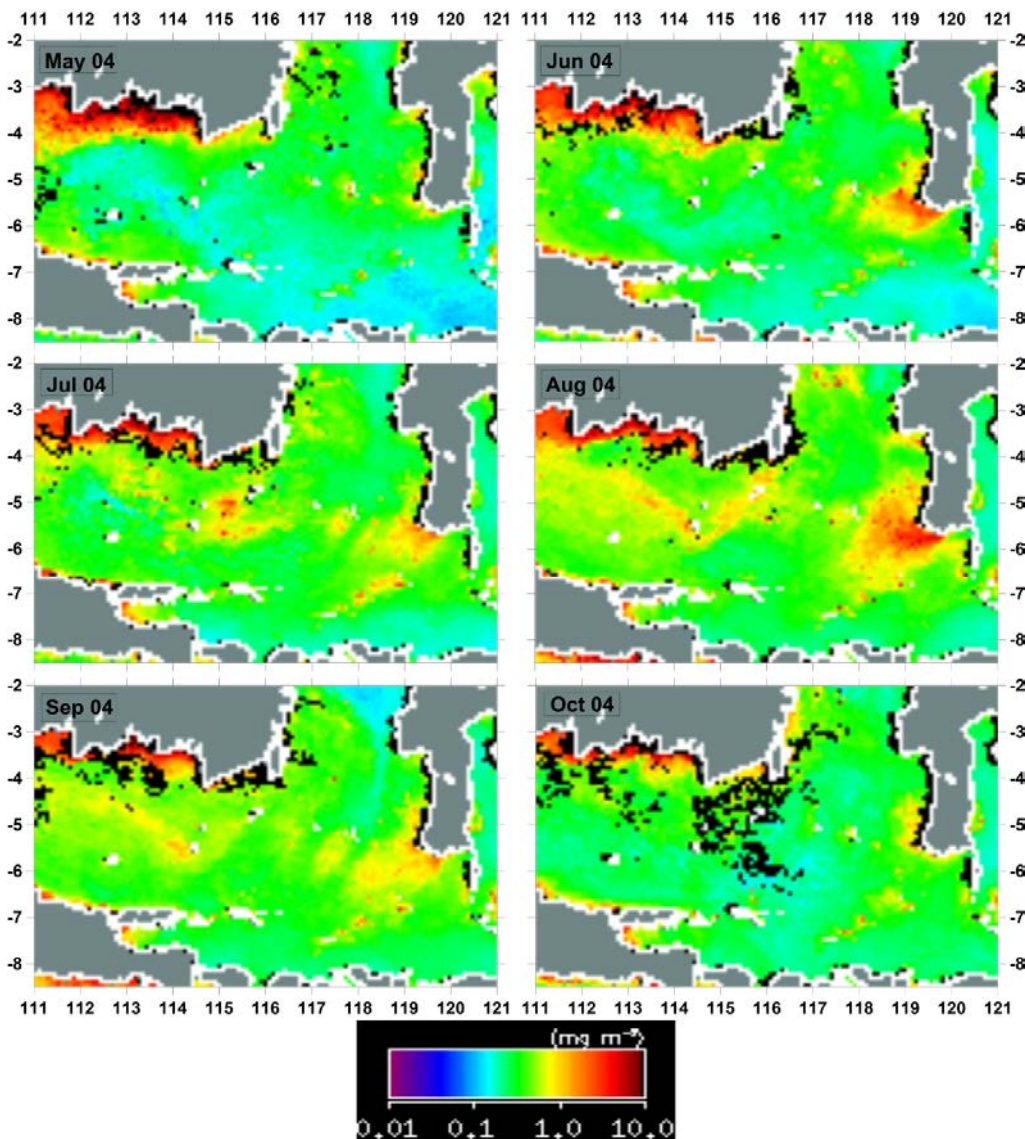


Fig. 8. Example of spatial monthly mean Chl-a distribution of during east season (top and middle panels) and second transitional season (bottom panel).

### 3.3. Interannual Variability of SST and Chlorophyll-a Concentration

Interannual variability of SST and Chl-a were analysed by comparing the monthly mean SST and Chl-a data in each season between non-ENSO months vs. ENSO months. From this analyses, we found a significant interannual variability of monthly mean SST and Chl-a between non-ENSO months vs. ENSO months. For the four selected sampling areas, in general, monthly mean SST values were relatively lower during ENSO months than during non-ENSO months at the end of east season (August) and second transitional season (September and October) (Fig. 9). However, the variabilities were only significantly different at the sampling area1 and sampling area4. Meanwhile, at the sampling area 2 and sampling area 3, the variabilities were within the standard deviation (see Fig. 8). This results indicated that upwelling events were intensified during ENSO years in August, September, and October and this was

evident from satellite data during ENSO years of 2003, 2004, 2006, and 2014.

Based on monthly mean Chl-a data, the results showed that only sampling area 1 experienced a significant interannual variability between ENSO and non-ENSO months of August, September, and October. During these months, monthly mean Chl-a values were slightly higher during ENSO months than during non-ENSO months (Fig. 10). This event was affected by upwelling intensification during ENSO months since the ESE wind speed during the ENSO months was relatively higher than during non-ENSO months. For the other three selected sampling areas, however, there were no significant interannual variabilities in monthly mean Chl-a between ENSO months and non-ENSO months.

### 3.4. Factors affecting variability of SST and chlorophyll-a concentration

In general, SST variability is affected by meteorological conditions (precipitation, evaporation, air humidity, air temperature, wind speed, and solar radiation intensity) and oceanographic processes (current, front, and upwelling). Chlorophyll-a concentration variability is affected by the variability of SST, rainfall, nutrients, current, and solar radiation intensity. Therefore, both SST and chlorophyll-a concentration variabilities usually follow a seasonal pattern (Nontji, 2005). In this study, we analysed the factors affecting the variability of SST and chlorophyll-a concentration based on wind, precipitation, and other meteorological factors such as El Nino Southern Oscillation (ENSO).

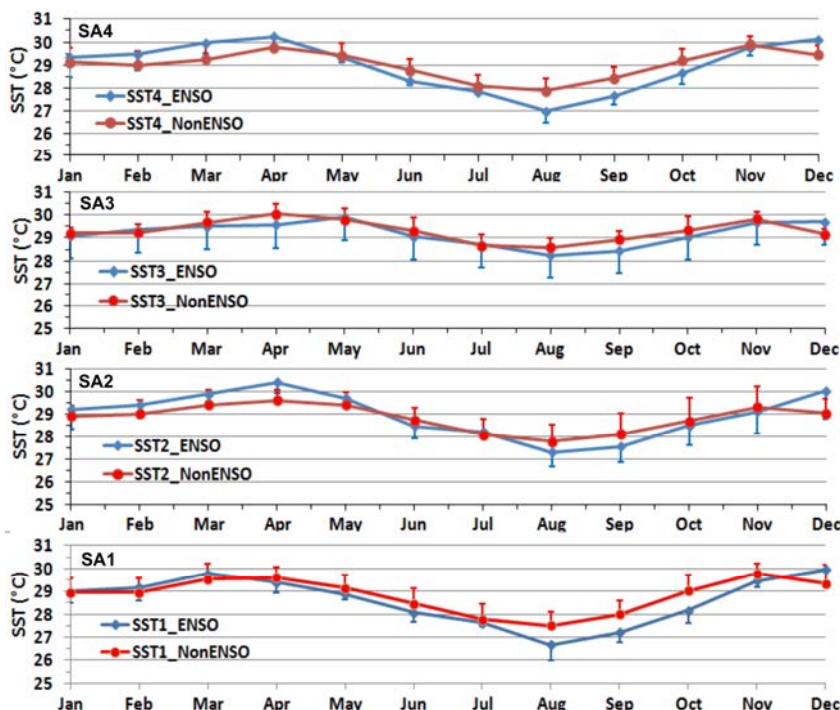


Fig. 9. Monthly mean SST plot during ENSO years (blue) vs. non-ENSO years (red) of the four selected sampling areas.

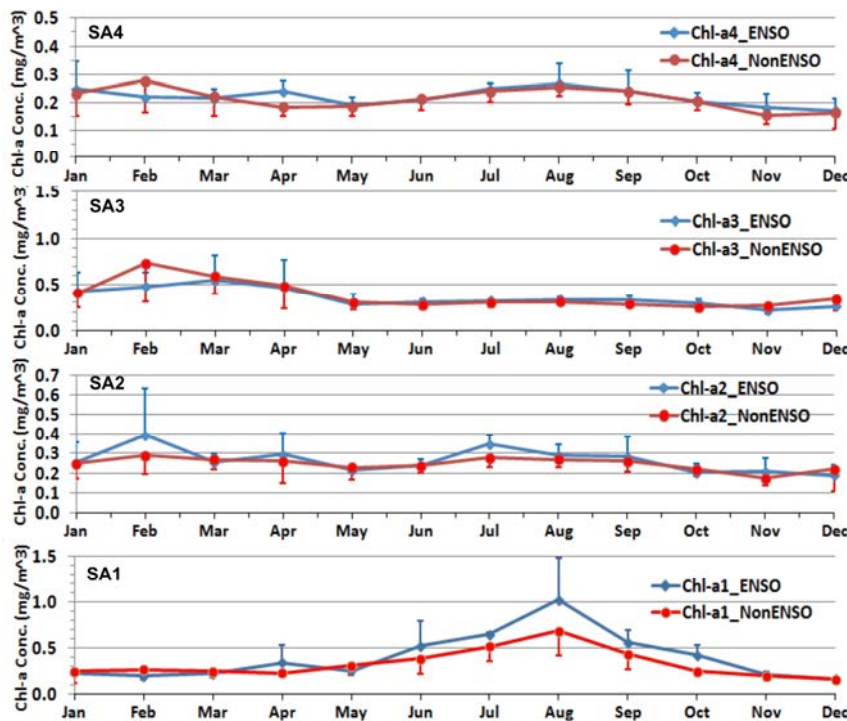


Fig. 10. Monthly mean Chl-a concentrations plot during ENSO years (blue) vs. non-ENSO years (red) of the four selected sampling areas. Note that the y-axis in each sampling areas do not have the same scale.

#### Wind

Wind patterns over Indonesian region changed within the season specifically between west and east seasons. Westerly or northwesterly wind generally blew over Indonesian region during the west season (November–February), while easterly or southeasterly wind generally blew during the east season (May–August). For the first transitional season (March–April) and second transitional season (October–November), wind normally blew in irregular patterns [2, 17, 27].

Based on 17 years of monthly mean wind data extracted from sampling areas 1, we found that in general east-southeasterly (ESE) wind blew over south of Makassar Strait started in April up to September with a gradually increase speed from the month of April, reach its maximum in August, and then gradually decrease the speed until September. The maximum speed of ESE wind was 7.01 m/s (August, 2008) and the minimum was 1.76 m/s in October 2000. Meanwhile, west-northwesterly (WNW) wind blew over the region started in December up to March with the maximum speed in January. The minimum speed of WNW occurred in November 2003 of 0.24 m/s and the maximum occurred in January 2008 of 6.45 m/s. During the month of October, the wind direction was generally from northwest (NW) and during the month of November generally from north-northwest (NNW) direction with relatively low wind speed (see Fig. 2).

Based on the monthly mean SST anomalies and x-component wind speed analyses, we found that monthly mean SST variabilities were mostly affected by variabilities of x-component wind speed. On the monthly basis analyses, we found that when the ESE winds blew over the south of Makassar Strait, the monthly mean SST anomalies tended to be negative. However, if the wind speed was <5.0 m/s, then the monthly mean SST anomalies were within  $-0.5^{\circ}\text{C} < \text{SST anomaly} < 0^{\circ}\text{C}$ . This condition can be identified as initiation stage of an upwelling event. In general, if the ESE wind speed was >5.0 m/s, then 90% of the monthly mean SST anomalies were  $<-0.5^{\circ}\text{C}$  (the negative anomaly border for upwelling event). This condition can be identified as a fully developed upwelling event. Meanwhile, when the WNW or NW winds blew over the region, the monthly mean SST anomalies tended to be in positive values. The maximum value of positive anomalies occurred when WNW or NW wind speed reached its lowest value that normally occurred in April or November (see Fig 2).

To see how much wind factor contributed into monthly mean SST anomalies, we performed polynomial fit regression analyses between monthly mean SST anomalies and monthly mean x-component winds. The result showed that 59% ( $R^2=0.59$ ) variabilities of monthly mean SST were caused by the variabilities of monthly mean x-component winds.

We delineated upwelling events based on the values of monthly mean SST anomaly for sampling area1 when ESE wind blew over the study region (May–October) i.e.,  $0 > \text{SST anomaly} > -0.5^\circ\text{C}$  as borders for upwelling initiation stage or termination stage and  $\text{SST anomaly} < -0.5^\circ\text{C}$  as a border for fully developed stage of an upwelling event. Based on analyses of SST anomalies and ESE wind speed in the sampling area1, we found that upwelling events initiation started in May with 23.53% (4/17 events) frequency, in June with 17.65% (3/17 events) frequency, and in July with 11.76% (2/17 events) frequency. A fully developed stage started in May with 6% (1/17 event) frequency, in June with 58.82% (10/17 events) frequency, in July with 76.47% (14/17 events) frequency, and maximum in August with 94.12% (16/17 events) frequency. The upwelling event in general diminished in September and terminated at the end of October.

In general, the upwelling stage was controlled by the ESE wind speed. In this study, we found that an upwelling event reached its full stage when the ESE wind speed  $> 5.0 \text{ m/s}$ . The maximum upwelling event (August) occurred when the ESE wind speed reached its maximum speed. From this result, it was also revealed that an upwelling initiation or termination stage occurred when the ESE wind speed  $< 5.0 \text{ m/s}$ .

In the previous sub-chapter, we found that in general monthly mean SST values were relatively lower during ENSO months than in non-ENSO months specifically for the sampling area1 and sampling area4 when ESE wind blew over the region. To proof this finding, we analysed wind speed during ENSO months vs. non-ENSO months and we found that in general the wind speed during ENSO months was relatively higher than in non-ENSO months for the months of May–October when ESE wind blew the region (Fig. 11). The higher ESE wind speed produced higher Ekman surface current to the southwest direction causing larger and colder water from the deeper upwelled into the surface. This explained why during ENSO months, the intensity of upwelling event was in general relatively higher than during non-ENSO months.

During the late west season (February) and the early first transitional season (March), however, the WNW wind speeds were relatively lower during ENSO months than during non-ENSO months. However, this would not affect very much the variability of monthly mean SST values in the region. The WNW wind may intensify Ekman surface current toward northeast (NE) and downwelled water in the region.

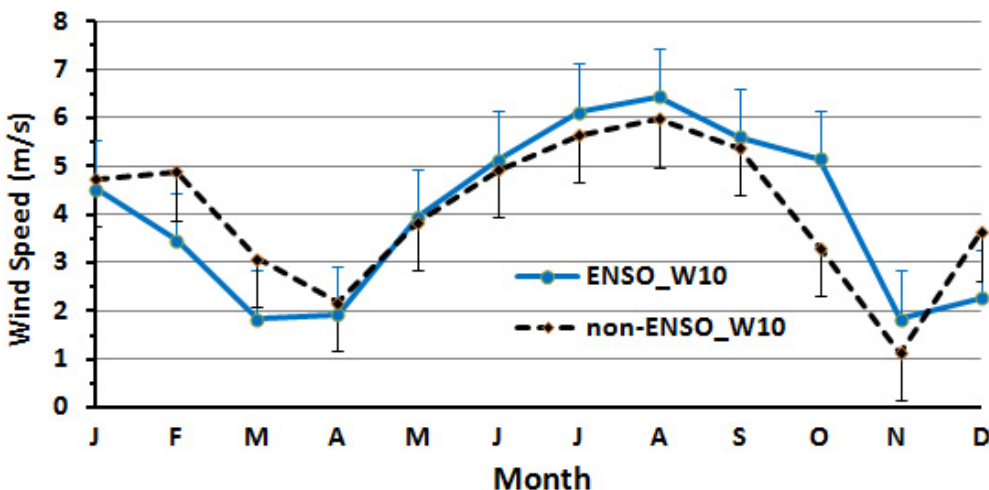


Fig. 11. Annual mean of wind speed during ENSO years and non-ENSO years extracted from sampling area 1

#### ■ Rainfall

Rainfall data were obtained from Paotere Meteorological Station, Makassar (the closest meteorological station into the sampling area1) for the period of January 1998 - December 2014. The rainfall data was then linked to the Chl-a data within the four selected sampling areas. Monthly mean rainfall of 17 year observations showed a clear

rainy and dry seasonal patterns. During the west season (November–February) and first transitional season (March–April), the south of Makassar Strait experienced a rainy season with average rainfall of 215.79–737.35 mm/month. Meanwhile, during the east season (May–August) and second transitional season (September–October), the region experienced a dry season with average rainfall of 10.83–81.83 mm/month (Fig. 12). In general, the maximum rainfall occurred in the months of January (west season) and the minimum rainfall occurred in August (east season). This was consistent with Hendon [28] and Wyrtki [17] that the fluctuation of the monthly rainfall in Indonesia was affected by the monsoonal wind patterns. During the west season, the NW wind carried a lot of moisture over the South China Sea and produced high rainfall in Indonesian region. Meanwhile, during the east season, NE wind from Australian mainland brought dry air or little moisture and produced little rainfall in Indonesia.

In general, during the east season (low rainfall), in sampling area1, the monthly mean Chl-a increased to a maximum value (Fig. 13). This result indicated that the increase of monthly mean Chl-a during the east season was not related to rainfall or nutrients input from mainland but solely due to the upwelling event in the region. For sampling area3, it was clear that there was no upwelling impact in this region since during the east season (low rainfall) the monthly mean Chl-a was also minimum. In this region, it was also clear that the maximum monthly mean Chl-a occurred after maximum rainfall. This indicated that the monthly mean Chl-a in the northern site of study region was mostly affected by local input of riverine freshwater and the rainfall variability.

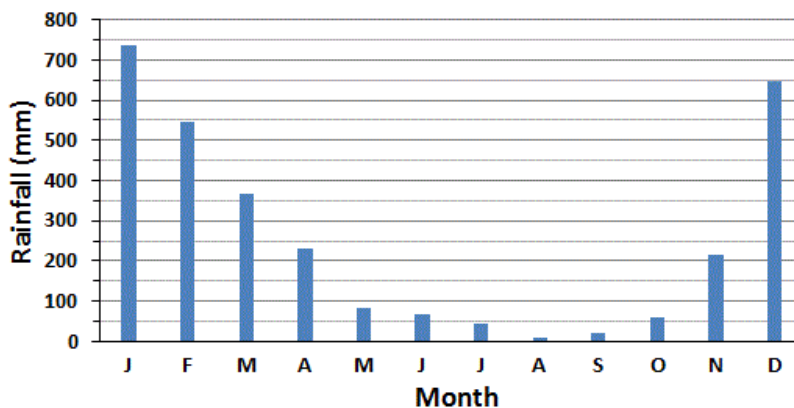


Fig. 12. Monthly mean rainfall of 17 years time period at the Paotere Meteorological Station.

#### 4. Conclusion

In general, the variability of monthly mean SST values showed a clear seasonal pattern with relatively high (positive anomalies) values during the west season (November–February) and first transitional season (March–April), while relatively low (negative anomalies) values during the east season (May–August) and second transitional season (September–October). The monthly mean SST variability seemed to be mostly affected by monsoonal wind speed and directions.

The ESE wind play a major role in an upwelling initiation ( $0 > \text{SST anomaly} > -0.5$ ) when wind speed of  $< 5 \text{ m/s}$ , and became a fully developed stage of an upwelling event ( $\text{SST anomaly} < 0.5^\circ\text{C}$ ) when wind speed of  $> 5 \text{ m/s}$ . Of the 17 years time period, the variability of monthly mean SST values ranged between  $25.7^\circ\text{C}$  and  $30.89^\circ\text{C}$ . Meanwhile, the variability of monthly mean Chl-a concentrations showed no similar seasonal patterns for the four selected sampling areas. For the sampling areas1 (region near to the southern tip of Sulawesi island), the variability of monthly mean Chl-a was coherently the opposite seasonal pattern of monthly mean SST variability. This indicated that variability of monthly mean Chl-a concentrations in sampling area1 was mostly affected by the variability of upwelling event. For the sampling area 3 (the northern site of the study region), the variability of Chl-a seemed to be affected by the variability of local riverine freshwater input and rainfall but not the upwelling event in the south of Makassar Strait.

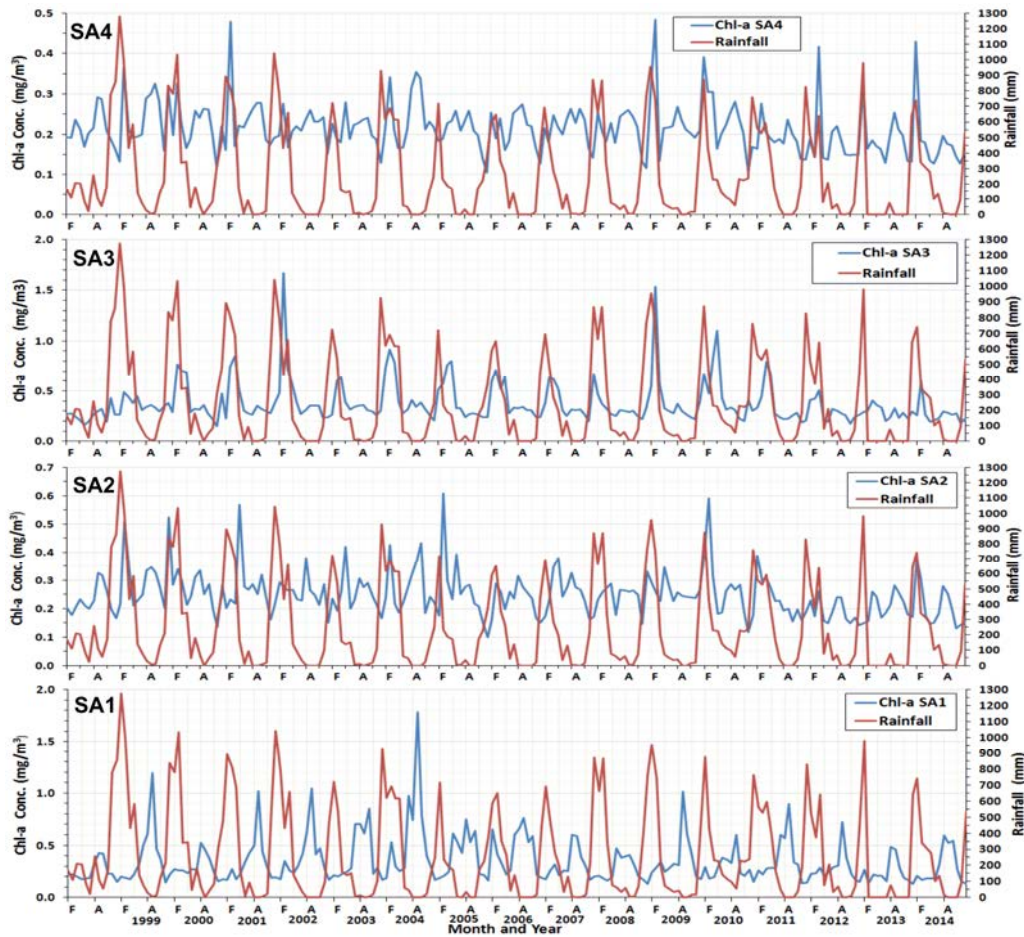


Fig. 13. Monthly mean Chl-a and rainfall fluctuation of the four selected sampling areas showing no clear relationship between Chl-a and the rainfall in sampling area 1, 2, and 3 but some positive relationship in the sampling area 3.

An upwelling initiation typically occurred in early May when ESE wind speed was at <5 m/s, a fully developed upwelling event usually occurred in June when ESE wind speed reached >5 m/s, whereas the largest upwelling event always occurred in August of each year. Upwelling event generally diminish started in September and terminated in October. At the time of the maximum upwelling events (August), the formation of upwelling could be observed up to about 330 km toward the southwest of the southern tip of the Sulawesi island. Interannually, El Niño Southern Oscillation (ENSO) intensified the upwelling event during the east season through enhancement of the ESE wind speed.

#### Acknowledgments

This research was partly supported by Directorate General of Higher Education, Ministry of Education and Culture, Republic of Indonesia on IPB Strategic Research grant fiscal year of 2014 with MAK code of 2013.109.52-1119,-1211,-1213,-4211. We would like to thank NASA, ECMWF, and BMKG for providing satellite and in situ data for this research. We also thank to the NASA GES DISC for providing “Giovanni online data system for analyses and visualizations” to be used in this paper. We would like to express our gratitude to Mr. Muhammad Iqbal for helping reproducing some graphs in this paper. We appreciated comments from reviewers to improve the quality of this paper.

## References

1. Atmadipoera, A.S. and P. Widystuti, *A numerical modeling study on upwelling mechanism in South of Makassar Strait*. J. of Tropical Marine Science and Technology. 2014;**6**(2): 355-371.
2. Habibi, A., R.Y. Setiawan, and A.Y. Zuhdy, *Wind-driven coastal upwelling along South of Sulawesi Island*. Indonesian J. of Marine Science, 2010. **15**(2): 115-118.
3. Wheeler, M.C. and J.L. McBride, *Australian-Indonesian monsoon*. In: *Intraseasonal Variability in the Atmosphere-ocean System*, edited by W.K.M. Lau and Waliser, D.E. chap. 5, 2005. pp. 125–173, Springer, Berlin, doi:10.1007/3-540-27250-X\_5.
4. Susanto, et al., *Variability of Indonesian throughflow within Makassar Strait, 2004–2009*. J. Geophys. Res. 2012. 117. C09013. doi:10.1029/2012JC008096.
5. Gordon, et al., *The Indonesian throughflow during 2004-2006 as observed by the INSTANT program in “modeling and observing the Indonesian throughflow”*, Guest Editors: Gordon, A.L. and V.M. Kamenkovich. Dynamics of Atmosphere and Oceans, 2010. 50: p. 115-128.
6. Gordon, et al., *Makassar Strait throughflow, 2004 to 2006*. Geo Res Lett., 2008. 35. L24605. doi:10.1029/2008GL036372.
7. Susanto, R.D. and A.L. Gordon, A.L., *Velocity and transport of the Makassar Strait throughflow*. J. Geophys. Res., 2005. 110, C01005, doi:10.1029/2004JC002425.
8. Gordon, A.L., *Oceanography of the Indonesian seas and their throughflow*. Oceanography; 2005. 18: p. 14–27, doi:10.5670/oceanog.2005.01.
9. Gordon, A.L., R.D. Susanto, and K. Vranes, *Cool Indonesian throughflow as a consequence of restricted surface layer flow*. Nature; 2003. 425: p. 824–828, doi:10.1038/nature02038.
10. Syahdan, et al., *Variability of surface chlorophyll-a in Makassar Strait - Java Sea, Indonesia*. IJSBAR, 2014;**14**(2): 103-116.
11. Setiawan, R.Y. and H. Kawamura, *Summertime phytoplankton bloom in the South Sulawesi Sea*. IEEE J Sel Topics Appl Earth Observ., 2010. p. 1939-1404. doi:10.1109/JSTARS.2010.2094604.
12. Susanto, et al., *Intraseasonal variability and tides in Makassar Strait*. Geophy. Res. Lett., 2000;27:1499-1502.
13. Saji, et al., *A dipole mode in the tropical Indian Ocean*. Nature, 1999;**401**: 360-363.
14. Afdal and S.H. Riyono, *Chlorophyll-a distribution and its relation to hydrology condition in South of Makassar Strait (in Bahasa)*. Oseanologi dan Limnologi di Indonesia, 2004;**36**: 69-82.
15. Hautala, et al., *Velocity structure and transport of the Indonesian throughflow in the major straits restricting flow into the Indian Ocean*. J. Geophys. Res., 2001;**106**: 19,527–19,546, doi:10.1029/2000JC 000577.
16. Meyers, G., R.J. Bailey, and A.P. Worby, *Geostrophic transport of Indonesian Throughflow Deep Sea Res.*, 1995;**42**(7): 1163–1174.
17. Wyrtki, K., *Physical oceanography of south east Asia Waters*. Naga Report, Vol 2. Scripps Institution of Oceanography La Jolla California. The University of California; 1961. 195p.
19. Atmadipoera, et al., *Characteristics and variability of the Indonesian Throughflow Water at the outflow Straits*, Deep Sea Research I., 2009;**56**:1942-1954.
20. Nontji, A., *Laut Nusantara*. Djambatan, Jakarta; 2005. 368p. *In Bahasa*.
21. Ilahude, A.G., *On the occurrence of upwelling in the South of Makassar Strait*. Mar. Res. Indonesia; 1970. 10:p. 3-53.
22. Ilahude, A.G., *On the factors affecting the productivity of the South of Makassar Strait*. Mar. Res. Indonesia, 1978;**21**: 81-107.
24. Acker, J.G. and G. Leptoukh, *Online analysis enhances use of NASA Earth Science Data*. Eos, Trans. AGU., 2007;**88**(2): 14-17.
25. O'Reilly, et al., *Ocean color chlorophyll-a algorithms for SeaWiFS, OC2 and OC4: Version*. In: Hooker, S.B & E. R. Firestone (eds.), *SeaWiFS postlaunch tech. report series, volume 11, SeaWiFS postlaunch calibration and validation analysis*, Part 3. Goddard Space Flight Center, Greenbelt, Maryland, NASA/TM-2000-206892, 2000;**11**: 9-23.
26. Kilpatrick, K.A., G.P. Podesta, and R.E. Evans, *Sea surface temperature global area coverage (GAC) processing version 4.0*, 1998. <http://www.rsmas.miami.edu/groups/rsrl/pathfinder/Algorithm> [23 September 2014].
27. Nababan, B., B. Hasyim, and H.L.N. Bada, *Variability dan validation of sea surface temperature estimated by Pathfinder Algorithm of NOAA-AVHRR satellite in the North Papua waters*. International J. of Remote Sensing and Earth Sciences, 2011;**8**: 25-31.
28. Tritel, H., *Understanding and forecasting ENSO*. 2010. <http://www.ncdc.noaa.gov/oa/rsad/ENinoresearchpaper.pdf>. [30 September 2014].
29. Hendon, H.H., *Indonesian Rainfall Variability: Impacts of ENSO and Local Air–Sea Interaction*. J. of Climate, 2003;**16**: 1775-1790.
30. Hackert, E.C. and S. Hastenrath, *Mechanisms of Java rainfall anomalies*. Mon. Wea. Rev., 1986;**114**: 745–757.
31. Ilahude, A.G. and A.L. Gordon, A.L., *Thermocline stratification within the Indonesia Seas*. J. Geophys. Res., 1996;**101**:12401-12409.
32. Wouthuyzen, S., *Upwelling study in Seram Sea and Banda Sea*, Oseanologi dan Limnologi di Indonesia, 2002;**36**: 17-35. *in Bahasa*.